Title
Effect of strain and thickness on the transition temperature of epitaxial FeRh thin-films

Journal
Applied Physics Letters, 111(17)

ISSN
0003-6951

Authors
Ceballos, A
Chen, Zhanghui
Schneider, O
et al.

Publication Date
2017-10-23

DOI
10.1063/1.4997901

Peer reviewed

Effect of strain and thickness on the transition temperature of epitaxial FeRh thin-films

A. Ceballos, Zhanghui Chen, O. Schneider, C. Bordel, Lin-Wang Wang, and F. Hellman

Citation: Appl. Phys. Lett. **111**, 172401 (2017); doi: 10.1063/1.4997901
View online: http://dx.doi.org/10.1063/1.4997901
View Table of Contents: http://aip.scitation.org/toc/apl/111/17
Published by the American Institute of Physics

Effect of strain and thickness on the transition temperature of epitaxial FeRh thin-films

A. Ceballos,[1] Zhanghui Chen,[2] O. Schneider,[3] C. Bordel,[3] Lin-Wang Wang,[2] and F. Hellman[2,3]
[1]*Department of Materials Science and Engineering, University of California Berkeley, Berkeley, California 94720, USA*
[2]*Materials Sciences Division, Lawrence Berkeley National Laboratory, Berkeley, California 94720, USA*
[3]*Department of Physics, University of California, Berkeley, Berkeley, California 94720, USA*

(Received 27 July 2017; accepted 9 October 2017; published online 23 October 2017)

The separate effects of strain and film thickness on the antiferromagnetic-to-ferromagnetic phase transition temperature of FeRh thin films by both experiment and density functional calculations were determined. Strain was introduced by epitaxial growth onto MgO, $SrTiO_3$, and $KTaO_3$ substrates. Film thicknesses below 15 nm substantially suppress the transition temperature, T*, to below room temperature in unstrained films. For strained films, tensile/compressive strain decreases/increases T*, respectively. $KTaO_3$ (001) substrates produce sufficient compressive strain to increase the transition temperature of 10 nm FeRh films above room temperature, which is useful for many proposed applications previously limited by the stabilization of the ferromagnetic state at small thicknesses. These results demonstrate that a judicious use of film thickness and substrate can be used to manipulate FeRh's transition temperature over a ~200 K range. *Published by AIP Publishing.* https://doi.org/10.1063/1.4997901

CsCl-ordered FeRh has attracted and sustained interest since 1938[1,2] due to its first-order magnetic phase transition from an antiferromagnetic (AF) to a ferromagnetic (FM) state when heated above a transition temperature (T*) of ≈350 K.[3,4] The FM phase has a collinear structure with 3.2 μ_B per Fe atom and 1.0 μ_B per Rh atom; the antiferromagnetic phase is of G-type with 3.1 μ_B per Fe atom and zero Rh moment.[5] The proposed applications include heat-assisted magnetic recording (HAMR) in an exchange-spring system coupled to a hard magnetic layer[6,7] and magnetic refrigeration due to the large entropy change at the AF-FM transition.[8,9]

In order to employ FeRh for magnetic media applications, thin films with well-defined transitions are required.[10,11] The reduced film thickness, however, leads to a lower transition temperature,[12,13] hindering the proposed storage applications. Accompanying this transition is an isotropic 1% lattice expansion, indicating that the magnetic order and the lattice of FeRh are strongly coupled. This has been further demonstrated by experiments using a ferroelectric substrate that induces strain either via an applied voltage[14] or by a structural phase transformation of the substrate.[15] Strain in FeRh films also causes a spin reorientation accompanying the AF-FM transition, as well as perpendicular anisotropy in the AF phase.[16] The effects of strain and thickness however have not been deconvolved.

In this study, we determine the separate effect of film thickness and strain from epitaxial growth of FeRh thin films deposited on substrates of varying lattice constants. The bulk FeRh lattice parameter is 2.985 Å in the AF state and 2.995 Å in the FM state. Strain arising from epitaxial growth is modulated by lattice mismatch between the film and substrate. Three substrates were used: MgO, $KTaO_3$ (KTO), and $SrTiO_3$ (STO) which are cubic with lattice parameters of 4.216 Å, 3.989 Å, and 3.905 Å, respectively. FeRh grows at an angle of 45 degree with respect to the substrate's [010] and [100] in-plane directions, so the effective lattice parameters of the substrates are 2.981 Å, 2.821 Å, and 2.761 Å. The effect of tensile strain was studied using a 100 nm thick film grown onto high energy ion-beam-assist-deposited (001) MgO (IBAD MgO), which was found to produce significant tensile strain.[16,17]

Epitaxial FeRh thin films of thicknesses 10, 15, 22, and 100 nm were grown by dc magnetron sputtering deposition from a single equiatomic FeRh target at a growth rate of 0.4 Å/s. The base pressure was 8×10^{-8} torr, and the growth pressure was 2 mtorr of Ar. Films were grown at 873 K and capped at room temperature with 3 nm of Pt, shown in previous work[18] to eliminate an interfacial FM phase that can form at the film/capping interface. The composition of all films was determined to be 48 at.% Fe/52 at.% Rh using energy dispersive X-ray spectroscopy.

Epitaxial relationships and lattice parameters were obtained from θ-2θ and ϕ scans with an X-ray diffractometer (XRD). The magnetic properties including the phase transition were determined using a superconducting quantum interference device (SQUID) magnetometer and a vibrating sample magnetometer (VSM). With the exception of the films grown on KTO, the magnetization (M) as a function of temperature was measured in a magnetic field of 5 T in the SQUID; this field decreases the transition temperature by –8 K/T.[4,16] The films on KTO were measured using a VSM since their full transition could not be captured due to SQUID's maximum temperature of 400 K. The magnetization as a function of temperature for these KTO samples was measured in a 1 T magnetic field.

Because there is substantial hysteresis associated with the first order AF-FM transition, which induces significant lattice expansion which is converted to strain due to the constraint of the substrate,[16] it is crucial to establish whether

samples are in the FM or AF state (and not in some mixed state) when M(H) or XRD is measured. To ensure this, a specific thermal and field history was used for each sample because of different T* and breadth of transition. For samples on MgO and STO, the samples were first cooled to 100 K (in zero field), and then, M(T) was measured from 100 to 400 K in a 5 T field. At 400 K, M(H) was measured, followed by M(T) from 400 to 100 K also in a 5 T field. The samples were then cooled to $T < 10$ K and subsequently warmed up to 300 K for removal (with both sequences done under zero field). At the end of this process, the 100 and 22 nm thick films on MgO and STO were fully in the AF state at room temperature, while the 15 and 10 nm thick films on MgO and STO were in a mixed state. To address this, the latter films were given an extra treatment involving heating to 400 K and then cooling from 400 to 300 K, both in a 5 T field. This results in the 10 and 15 nm thick films on MgO and STO being in the FM state at room temperature. The KTO samples instead were first cooled to 77 K in a liquid nitrogen bath, followed by the M(T) measurement in the VSM from 310 K to 500 K in a 1 T field. This history leads all samples on KTO to be fully in the AF state at room temperature. XRD (see supplementary material) determined the epitaxial relationship of all films to be (001) FeRh//(001) substrates and [100] FeRh//[110] substrates.

Figure 1(a) plots the transition temperatures T* of all films as a function of film thickness. The inset shows M(T) for a 22 nm film grown on MgO and indicates the transition temperatures upon cooling and heating in a 5 T field. Substantial hysteresis is seen in this transition, as discussed in the literature.[18,19] The transitions on heating (T^*_{AF-FM}) and cooling (T^*_{FM-AF}) are defined as the maximum of the first derivative of M(T). The transition width is defined as the difference between T^*_{AF-FM} and T^*_{FM-AF}. The transition temperature, T*, is then defined as the midpoint of T^*_{AF-FM} and T^*_{FM-AF}. The data are shown as measured in a 5 T field; for films on KTO, the 1 T measurements were corrected to 5 T by shifting T* down by 32 K. The zero-field T* is approximately 40 K higher than the 5 T T*.

Figure 1(a) shows that T* decreases sharply with the decreasing film thickness below 22 nm for all substrates. It also shows that T* depends on the substrate, which we will show below is due to a dependence on strain. For MgO and STO, T* drops below room temperature for films thinner than 15 nm, making this material impractical for many applications. However, FeRh films grown on KTO exhibit a considerably higher transition temperature such that even the thinnest films have T* above room temperature.

The width of the transition is presented in Fig. 1(b). Consistent with previous reports,[12,13] a broadening of the hysteresis is observed as the thickness of the film decreased. Previous work[19,20] has shown that AF domains nucleate preferentially at crystallographic defects with very little domain growth. In contrast, while the nucleation of the FM phase is also heterogeneous, it is then followed by significant growth of the domains. The data in Fig. 1(b) suggest that both the FM and AF phases are less easily nucleated and their domain walls are more easily pinned in thinner films, but a more careful study would be required to fully understand the nucleation and growth of both phases in these thin films.

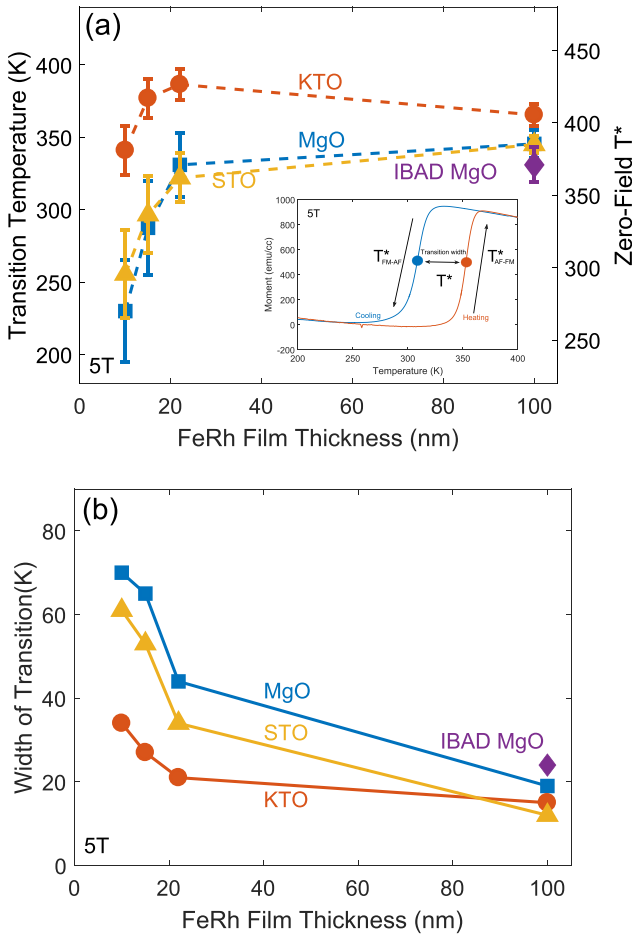

FIG. 1. (a) Transition temperature T* as a function of film thickness as recorded under a 5 T field (left axis) and adjusted to zero field (right axis). The decreasing thickness decreases the transition temperature across all films. The inset illustrates the magnetization as a function of temperature for a 22 nm FeRh film grown on MgO. The transition temperatures on heating and cooling are indicated, and their average equals the transition temperature T*. All magnetization measurements were done with the field along the plane of the film. (b) The width of the transition is the difference between the transitions on heating and cooling: T^*_{AF-FM} and T^*_{FM-AF}. All values are as recorded in a 5 T magnetic field except for films grown on KTO, which were measured in a 1 T field and then corrected to 5 T by subtracting 32 K.

The strain of all films was extracted from XRD measurements of the *c* and *a* lattice parameters using the (002) and off-axis (101) peaks, respectively. The ratios of c/a exceeding one correspond to films under compressive strain, while c/a below one corresponds to films under tensile strain. Specifically, films under compressive (tensile) strain correspond to films with an in-plane lattice parameter smaller (greater) than the bulk AF or FM lattice parameter at any given temperature.

Figure 2(a) shows that FeRh films grown on MgO and STO exhibit no strain with c/a values close to unity for all thicknesses, while films grown on KTO are compressively strained, and the film grown on IBAD MgO is tensilely strained. The films on KTO display decreasing strain with increasing film thickness, indicating the nucleation of misfit dislocations that release the strain as the film thickness is increased. The low strain of films grown on MgO is due to the close match of the lattice constant of MgO to that of FeRh. The low strain of films grown on STO, where significant strain was expected, is due to strain relaxation occurring

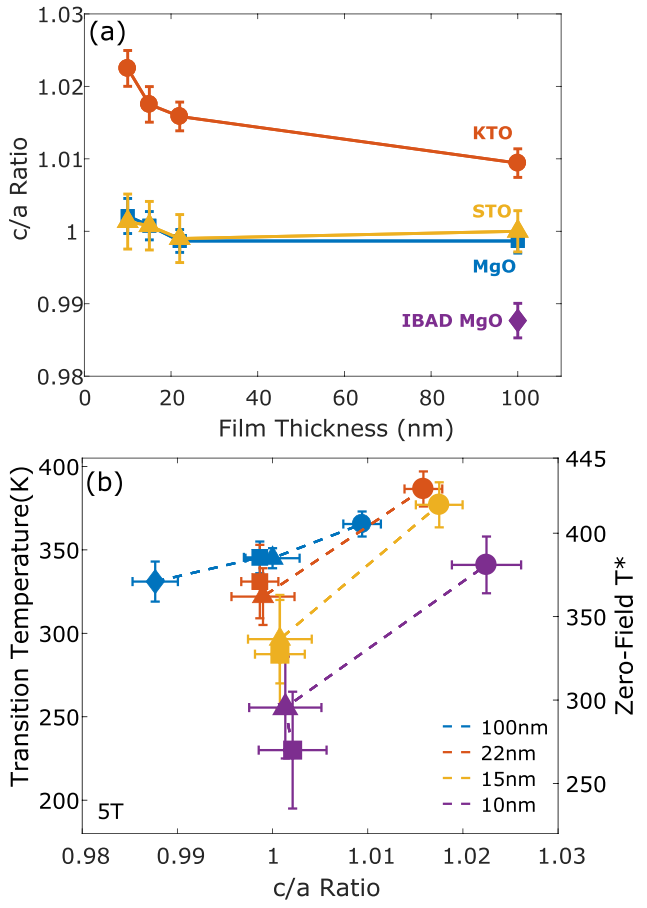

FIG. 2. (a) Thickness dependence of the strain. Films on KTO (IBAD MgO) are under compressive (tensile) strain. (b) The transition temperature recorded in 5 T (or corrected by 32 K for the KTO samples recorded in 1 T) as a function of the c/a ratio for films of fixed thicknesses. Tensile strain corresponds to $c/a < 1$ and compressive to $c/a > 1$. Films with the thickness 15 nm and below on MgO and STO had their c values corrected to the AF state by taking into account the 1% volume expansion (see supplementary material). Circles, squares, triangles, and diamond correspond to FeRh films grown on KTO, MgO, STO, and IBAD MgO, respectively.

in even the thinnest films. The fact that the strain state of films grown on MgO and STO is similar results in comparable transition temperatures as seen in Fig. 2(b). KTO however has lower lattice mismatch than STO, allowing for a higher critical thickness past which the nucleation of strain-relieving defects begins; this results in films that are somewhat compressively strained even at a film thickness of 100 nm. For the film on IBAD MgO, the strain is tensile, and the effect of tensile strain is seen to be a decrease in T*. Notably, the 10 nm film on KTO has T* comparable to the bulk.

Density functional theory (DFT) calculations (technical details are given in the supplementary material) allow simulation of the effect of strain and thickness on the electronic and magnetic properties of FeRh. We first perform the calculations for the bulk system at zero strain. These calculations yielded magnetic moments and spin polarized density of states (Fig. S1, supplementary material) that agree with literature values.[21,22] Next, the in-plane lattice parameters, $a = b$, were changed to emulate the strain produced by different substrates and the out-of-plane, c axis, was relaxed.

The total free energy of FM and AF states was then calculated, and then, the energy difference ΔE ($E_{FM} - E_{AF}$) per FeRh molecule between the two states was obtained. ΔE is the difference in free energy between the two states, and hence, the change in ΔE is proportional to the change in T*, as will be discussed below.

For $c/a = 1$, $\Delta E = 0.03$ eV/FeRh molecule. Since there is no entropy difference at zero temperature between the AF and FM states and the difference in Gibbs free energy at T* is zero, ΔS between the AF and FM states equals $\Delta E/T^*$ (for any c/a). This assumes that the non-zero temperature contribution is independent of c/a as discussed in the supplementary material. Since T_0^*, the transition temperature for $c/a = 1$, is ~350 K, it gives ΔS_0 at T_0^* for unstrained FeRh of 0.03 eV/FeRh molecule/350 K $\sim 3.25 \times 10^{20}$ eV/kg/K, about three times larger than the experimental value measured by latent heat or integration of C/T (see supplementary material) of 1.06×10^{20} eV/kg/K.[8] This discrepancy suggests an overestimation of ΔE which itself is very sensitive to the lattice parameters and computational methods;[5,23] however, this will not affect the qualitative discussion below nor the estimate of the shift in T* with strain, as discussed in the supplementary material. This ΔS_0 is due to vibrational, magnetic, and electronic degrees of freedom as discussed in previous work[8] which showed that all three contribute, but magnetic energy differences dominate. From this, assuming that the effect of strain on the excitation spectrum is smaller than its effect on the ground state energy, we approximate the change in T* as proportional to the change in ΔE with respect to the bulk using a Taylor expansion (see supplementary material): $T^* = T_0^*\left(1 + \frac{(\Delta E - \Delta E_0)}{\Delta E_0}\right)$, where $\Delta E_0 = 0.03$ eV/FeRh molecule. The result is shown in Fig. 3. For $c/a = 0.994$, the change in $\Delta E \approx -1.2$ meV, yielding a decrease of 14 K, consistent with the drop in T* with tensile strain. For $c/a > 1$, ΔE and T* increase, e.g., for $c/a = 1.011$ (close to the 100 nm film on KTO), the change in $\Delta E \approx 1.5$ meV, corresponding to an increase in T* of 17 K, consistent with the increased T* for compressive strain seen in the 100 nm film on KTO in Fig. 2(b).

Note that the above ΔE is calculated without considering spin anisotropy. The anisotropy energy (i.e., energy difference between the in-plane spin configuration and out-of-plane spin

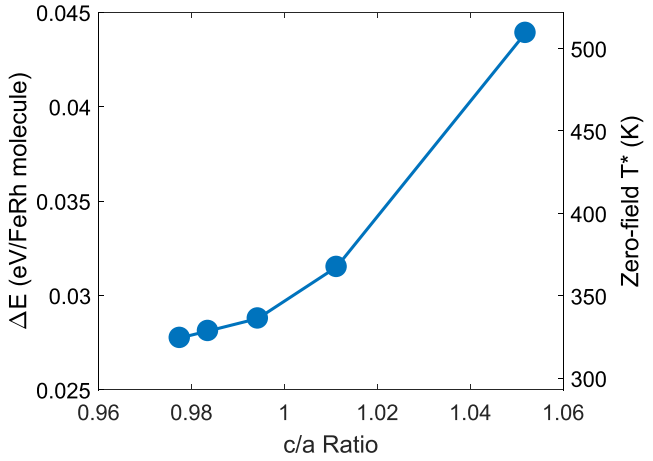

FIG. 3. The calculated energy difference ΔE ($E_{FM} - E_{AF}$) per FeRh molecule between the FM and the AF state vs c/a ratio for a bulk (thick) sample. The extraction of the zero-field transition temperature (right axis) is described in the main text. The c/a value in the x-axis uses the lattice parameter of the AF state for a selected value of $a = b$ after relaxation of c.

configuration) is in units of sub-meV,[16] much smaller than the changes in ΔE with strain. We also note that in the FM state, the in-plane spin configuration is preferred under tensile strain, while the out-of-plane spin configuration is preferred under compressive strain, and the reverse is seen for the AF state.[16] Thus, the anisotropy energy provides a small linear correction term (i.e., proportional to c/a) to ΔE.

DFT calculations also considered the effect of thickness. Calculations were performed on structures with two, four, six, and eight monolayers (ML), with each layer containing one layer of Fe atoms and one layer of Rh atoms. For each case, the energy and magnetic moments of the FM phase, G-type AF, and A-type AF were calculated; the A-type was included as it has been found to be more stable than the G-type for ultra-thin films.[24] For the FM phase, Fe has 3.17 μ_B and Rh about 1.05 μ_B for all thicknesses. For the G-type AF phase, Fe is 3.11 μ_B, lower than that of the FM state, and the moment for Rh is almost zero. For the A-type AF, the moment of Fe is about 3.14 μ_B, while the value of Rh is no longer zero but has a 0.87 μ_B spin-up moment in one layer and a 0.40 μ_B spin-down moment in the next layer, decreasing quickly to zero with increasing layers.

Figure 4 shows the energy difference (ΔE) between FM and AF states for different numbers of monolayers. The right axis is derived similar to Fig. 3 using a Taylor expansion in 1/N (see supplementary material). The G-type AF is the lowest energy state in the bulk, as known experimentally, with the higher energy FM state stabilized at high temperature (due to excitational, i.e., $T > 0$, entropy differences between the two states[8]). For thinner films, the energy difference is reduced and the FM state is the ground state at and below 6 layers. This dependence of the energy difference on thickness corresponds to a decreasing T* with the decreasing film thickness, as seen experimentally [Fig. 2(b)]. There is also a crossover between the G- and A-type AF states' energies at and below 2 layers, indicating that the A-type is more stable than the G-type in ultra-thin films (but in both cases, the FM state is more stable than the AF state).

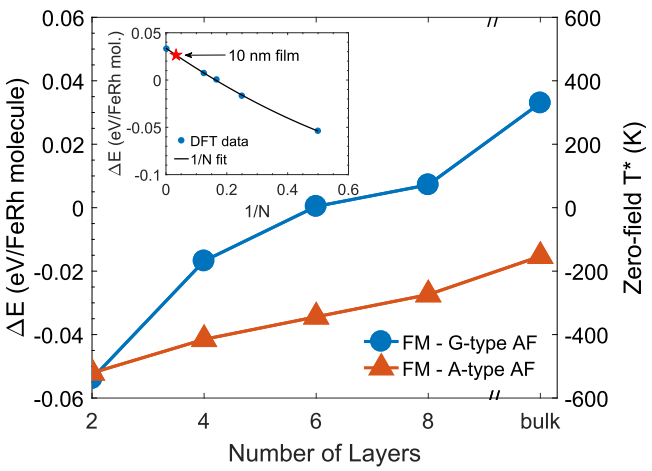

FIG. 4. The calculated energy difference ΔE ($E_{FM} - E_{AF}$) per FeRh molecule between the FM and the AF state (G-type and A-type) as a function of the number of monolayers (N). The extraction of the zero-field transition temperature (right axis) is described in the main text. T* below 0 K simply indicates that no transition exists, as the FM state has lower energy. The inset shows the 1/N fit used to extract T* for a 10 nm film.

A polynomial fit of ΔE vs the inverse of the thickness 1/N allows us to extract ΔE for a 10 nm film as seen in the inset of Fig. 4. Comparing this value to the bulk, we see a decrease in ΔE of 6.6 meV, predicting a T* of 273 K in zero field, very close to our zero field T* of 270 K and 296 K for our unstrained, 10 nm films on MgO and STO, respectively.

In conclusion, the transition temperature of epitaxial FeRh films is found to depend on both the thickness and strain; T* decreases with the decreasing film thickness and increases with the c/a ratio. For unstrained films, T* drops below room temperature for films below 15 nm in thickness. Tensile strain decreases T* and compressive strain increases T*. These effects are seen both experimentally and in DFT calculations, with excellent agreement between predicted and measured T*. For technological applications above room temperature, FeRh films epitaxially grown on KTO substrates are attractive candidates for magnetic storage applications as even 10 nm films possess a T* comparable to that of bulk FeRh.

See supplementary material for a table of extracted lattice parameters, transition temperatures, XRD spectra, and details on the implementation of DFT calculations.

This work was supported by the Director, Office of Science, Office of Basic Energy Sciences, Materials Sciences and Engineering Division, U.S. Department of Energy, under Contract No. DE-AC02-05-CH11231 within the Nonequilibrium Magnetic Materials Program (KC2204). A.C. acknowledges support by the National Science Foundation under Grant No. DGE 1106400.

[1]M. Fallot, Ann. Phys. (Leipzig) **11**, 291 (1938).
[2]M. Fallot and R. Horcart, Rev. Sci. **77**, 498 (1939); **77**, 291 (1939).
[3]V. L. Moruzzi and P. M. Marcus, Phys. Rev. B **46**, 2864 (1992).
[4]S. Maat, J.-U. Thiele, and E. E. Fullerton, Phys. Rev. B **72**, 214432 (2005).
[5]L. M. Sandratskii and P. Mavropoulos, Phys. Rev. B **83**, 174408 (2011).
[6]J.-U. Thiele, S. Maat, and E. E. Fullerton, Appl. Phys. Lett. **82**, 2859 (2003).
[7]J. U. Thiele, S. Maat, J. L. Robertson, and E. E. Fullerton, IEEE Trans. Magnetics **40**, 2537 (2004).
[8]D. W. Cooke, F. Hellman, C. Baldasseroni, C. Bordel, S. Moyerman, and E. E. Fullerton, Phys. Rev. Lett. **109**, 255901 (2012).
[9]E. Stern-Taulats, A. Gràcia-Condal, A. Planes, P. Lloveras, M. Barrio, J.-L. Tamarit, S. Pramanick, S. Majumdar, and L. Mañosa, Appl. Phys. Lett. **107**, 152409 (2015).
[10]Q. J. Yap, J. J. Qiu, P. Luo, J. F. Ying, G. C. Han, D. E. Laughlin, J.-G. Zhu, T. Kanbe, and T. Shige, J. Appl. Phys. **116**, 043902 (2014).
[11]T. J. Zhou, K. Cher, J. F. Hu, Z. M. Yuan, and B. Liu, J. Appl. Phys. **111**, 07C116 (2012).
[12]I. Suzuki, T. Koike, M. Itoh, T. Taniyama, and T. Sato, J. Appl. Phys. **105**, 07E501 (2009).
[13]G. C. Han, J. J. Qiu, Q. J. Yap, P. Luo, D. E. Laughlin, J. G. Zhu, T. Kanbe, and T. Shige, J. Appl. Phys. **113**, 17C107 (2013).
[14]R. Cherifi, V. Ivanovskaya, L. Phillips, A. Zobelli, I. Infante, E. Jacquet, V. Garcia, S. Fusil, P. Briddon, N. Guiblin, A. Mougin, A. Unal, F. Kronast, S. Valencia, B. Dkhil, A. Barthelemy, and M. Bibes, Nat. Mater. **13**, 345 (2014).
[15]I. Suzuki, M. Itoh, and T. Taniyama, Appl. Phys. Lett. **104**, 022401 (2014).
[16]C. Bordel, J. Juraszek, D. W. Cooke, C. Baldasseroni, S. Mankovsky, J. Minár, H. Ebert, S. Moyerman, E. E. Fullerton, and F. Hellman, Phys. Rev. Lett. **109**, 117201 (2012).
[17]D. W. Cooke, F. Hellman, J. R. Groves, B. M. Clemens, S. Moyerman, and E. E. Fullerton, Rev. Sci. Instrum. **82**, 023908 (2011).

[18]C. Baldasseroni, G. K. Pálsson, C. Bordel, S. Valencia, A. A. Unal, F. Kronast, S. Nemsak, C. S. Fadley, J. A. Borchers, B. B. Maranville, and F. Hellman, J. Appl. Phys. **115**, 043919 (2014).
[19]C. Baldasseroni, C. Bordel, A. X. Gray, A. M. Kaiser, F. Kronast, J. Herrero-Albillos, C. M. Schneider, C. S. Fadley, and F. Hellman, Appl. Phys. Lett. **100**, 262401 (2012).
[20]C. Baldasseroni, C. Bordel, C. Antonakos, A. Scholl, K. H. Stone, J. B. Kortright, and F. Hellman, J. Phys.: Condens. Matter **27**, 256001 (2015).
[21]S. Polesya, S. Mankovsky, D. Ködderitzsch, J. Minár, and H. Ebert, Phys. Rev. B **93**, 024423 (2016).
[22]J. Kudrnovskỳ, V. Drchal, and I. Turek, Phys. Rev. B **91**, 014435 (2015).
[23]R. Y. Gu and V. P. Antropov, Phys. Rev. B **72**, 012403 (2005).
[24]S. J. May, P. Ryan, J. Robertson, J.-W. Kim, T. S. Santos, E. Karapetrova, J. L. Zarestky, X. Zhai, S. Te Velthuis, J. Eckstein *et al.*, Nat. Mater. **8**, 892 (2009).